Physics and Imaging in Radiation Oncology 20 (2021) 56–61

Contents lists available at ScienceDirect

Physics and Imaging in Radiation Oncology

journal homepage: www.sciencedirect.com/journal/physics-and-imaging-in-radiation-oncology

First clinical evaluation of breathing controlled four-dimensional computed tomography imaging

Juliane Szkitsak [a,b], René Werner [c], Susanne Fernolendt [b,d], Annette Schwarz [b,d], Oliver J. Ott [a,b], Rainer Fietkau [a,b], Christian Hofmann [d,1], Christoph Bert [a,b,*,1]

[a] Department of Radiation Oncology, Universitätsklinikum Erlangen, 91054 Erlangen, Germany
[b] Friedrich-Alexander-Universität Erlangen-Nürnberg, 91054 Erlangen, Germany
[c] University Medical Center Hamburg-Eppendorf, 20246 Hamburg, Germany
[d] Siemens Healthcare GmbH, 91301 Forchheim, Germany

ARTICLE INFO

Keywords:
4DCT
Motion artifacts
Respiratory motion

ABSTRACT

Background and Purpose: Four-dimensional computed tomography (4DCT) has become an essential part of radiotherapy planning but is often affected by artifacts. A new breathing controlled 4DCT (i4DCT) algorithm has been introduced. This study aims to present the first clinical data and to evaluate the achieved image quality, projection data coverage and beam-on time.

Material & Methods: The analysis included i4DCT data for 129 scans of patients with thoracic tumors. Projection data coverage and beam-on time were evaluated. Additionally, image quality was exemplarily discussed and rated by ten clinical experts with a 5-score-scale for 30 patients with large variations in their breathing pattern ('challenging subgroup'). Rated images were reconstructed amplitude- and phase-based.

Results: Expert scoring revealed that 78% (amplitude-based) and 63% (phase-based) of the challenging subgroup were artifact-free (rating $\geq$4). For the entire cohort, average beam-on time per couch position was 4.9 $\pm$ 1.6 s. For the challenging subgroup, time increased slightly but not significantly compared to the remaining patients (5.1 s vs. 4.9 s; $p = 0.64$). Median projection data coverage was 93% and 94% for inhalation and exhalation, respectively, for the entire cohort. The comparison for the subgroup and the remaining patients revealed a small but significant decrease of the median coverage values for the challenging cases (inhalation: 90% vs. 94%, $p = 0.02$; exhalation: 93% vs. 94%, $p = 0.02$).

Conclusions: This first clinical evaluation of i4DCT shows very promising results in terms of image quality and projection data coverage. The results agree with and support the results of previous i4DCT phantom studies.

1. Introduction

Four-dimensional computed tomography (4DCT) has become an essential component in radiotherapy planning of tumors subject to respiratory motion, like lung or liver tumors [1,2]. 4DCT imaging has proven to be beneficial for delineation of internal target volumes [3–5] or selecting breathing phases for gated radiotherapy [6,7].

To achieve adequate 4DCT image quality, a constant relationship between respiratory signal and internal anatomical motion as well as sufficient projection data for reconstruction of phase images at all desired breathing states must be given. Additionally, the patient has to breathe regularly [8]. Violation of these assumptions due to irregular breathing leads to breathing-related artifacts [9–18] such as missing data or interpolation artifacts and sorting artifacts (double or incomplete structures) [19]. As a consequence, delineation errors [10,13,17,20] and incorrect dose calculation may occur [2,17], potentially leading to unfavorable treatment outcome [21].

To minimize the impact of patient breathing irregularity on image quality, different approaches have been developed over the past years. Pan et al. [11] proposed a 4DCT technique that allowed to retrospectively remove certain parts of the breathing signal and its associated projection data if breathing irregularities occur. In a study by Keall et al. [15], CT data acquisition is controlled by a real-time analysis of the respiratory curve and is triggered with regard to the breathing curve

* Corresponding author at: Universitätsklinikum Erlangen, Department of Radiation Oncology, Universitätsstraße 27, 91054 Erlangen, Germany.
E-mail address: Christoph.Bert@uk-erlangen.de (C. Bert).
[1] Contributed equally.

https://doi.org/10.1016/j.phro.2021.09.005
Received 11 June 2021; Received in revised form 17 September 2021; Accepted 17 September 2021

regularity. If breathing irregularities occur, the acquisition is paused until the patient breathes regularly again. A respiratory displacement and velocity-based prospective cine CT method was published by Langer et al. [17]. If the displacement and the velocity of the respiratory signal are at the same time within a certain pre-defined tolerance, the data acquisition is triggered. Castillo et al. [20] further analyzed the effects of three alternative methods for artifact reduction. Besides data oversampling and beam gating, rescanning of sections that were acquired during breathing irregularities was investigated.

Recently, Werner et al. proposed the so-called "intelligent 4DCT (i4DCT) algorithm" [22], a 4DCT scan mode, that is controlled by the patient's breathing. By online analysis of the patient's breathing signal, the length of the CT beam-on/-off periods is adapted during scanning. This approach has been shown to result in a significant reduction of 4DCT artifacts in *in-silico* investigations as well as in phantom measurements [22–24]. Yet, clinical i4DCT data, i.e. real patient data, have so far not been evaluated and presented.

The aim of the current work was therefore the evaluation of the hypothesis that better image quality and a reduction of typical 4DCT artifacts could be achieved compared to previously available algorithms, by using i4DCT. For this purpose, clinical data was evaluated in terms of image quality, beam-on time (as a proxy for dose exposure) and projection data coverage.

2. Materials and methods

2.1. Breathing controlled 4DCT algorithm

The main idea of breathing controlled 4DCT lies in automated adaption of the CT data acquisition to the patient's breathing pattern. The algorithm consists of two steps. The first step is an initial learning period to acquire a patient-specific reference breathing cycle. Based on this data, the scan parameters (e.g. gantry rotation time, estimated scan duration) are adjusted automatically such that each patient is assigned with an appropriate starting set of scanning parameters.

The second step is a sequence scanning method, guided by an online breathing signal analysis. By reaching a pre-defined degree of similarity between the breathing curve during scanning and the reference breathing cycle, the X-ray beam is switched on immediately prior to the patient-specific end-inspiration peak. The reference breathing cycle is initially established during step 1 and updated during scanning. Projection data and the breathing signal are then continuously acquired and examined with regard to the coverage of the acquired projection data. The concept of projection data coverage is described in more detail below. When sufficient coverage for all breathing states is achieved, the scan at the defined z-position is terminated. The table is then moved to the next z-position. The described steps are repeated until the whole scanning range is covered. A video of the scanning process described in this section can be found in the supplementary material. Detailed information about the algorithm and its parameters were published in the concept paper of Werner et al. [23].

2.2. Breathing motion surrogate signal acquisition

In our institution, the patient's breathing curve during the CT scan was acquired by the Varian 'respiratory gating for scanners' system (RGSC, version 1.1.25.0, Varian Medical Systems, Inc. Palo Alto, CA). This system mainly consists of a couch-mounted infrared (IR) camera and a marker block with passive reflectors, positioned on either the patient's abdomen or thorax. The camera emits IR light and detects the reflection by passive markers to calculate the position. Subsequently, the collected data of the patient's breathing curve is transmitted to the CT scanner in real-time and used for online analysis as part of the breathing controlled 4DCT algorithm.

2.3. 4DCT acquisition and image reconstruction

4DCT data was acquired using a SOMATOM go.Open Pro scanner (Siemens Healthcare, Forchheim, Germany) that offers the first commercially available breathing control 4DCT implementation (product name: "Direct intelligent 4DCT", referred to as i4DCT). The 4DCT scans were part of our clinical protocol for tumors with respiratory-related motion. The default setting for the CT scan was a tube voltage of 120 kV, 64 × 0.6 mm collimation and a couch increment of 0.9 × 64 × 0.6 mm. The gantry rotation time was automatically adapted to the patient's breathing frequency. The raw data was reconstructed as multiphase images (i.e., ten 3D CT images at different breathing phases) with a slice thickness of 3 mm and a semi-smooth kernel Qr40.

2.4. Patient cohort

The analysis includes a collective of 129 scans of patients treated in the period from 10/2019 to 05/2020. To collect a patient cohort as homogeneous as possible, only patients with thoracic tumors were included. The collective included 51/129 (40%) women and 78/129 (60%) men. The mean age was 66 ± 10 years. Further details are given in Table 1.

All CT scans used for the study were acquired as part of clinical routine. All procedures performed were in accordance with the ethical standards of the institutional research committee and with the 1964 Helsinki declaration and its later amendments. Patient consent was not required for this retrospective study per institutional policy.

Table 1
Patient collective (N = 129) details. Lung and mediastinum patients were treated normo-fractionated with 1.8Gy in ≥28 fractions or stereotactic with a dose per fraction ≥3 Gy and fractions ≤15. Ribs were treated with a simultaneous integrated boost (12 × 3 Gy/ 4 Gy) or 10 × 3 Gy.

	n	*(%)*
Age		
<50	7	(5%)
50–59	19	(15%)
60–69	58	(45%)
70–79	30	(23%)
>79	15	(12%)
Sex		
female	51	(40%)
male	78	(60%)
Tumor location		
lung/mediastinum	111	(86%)
stereotactic	63	(49%)
normo-fractionated	48	(37%)
ribs	11	(9%)
other	7	(5%)

2.5. Selection of exemplary cases for illustration

The image quality achieved by the algorithm was presented and exemplary discussed using four examples of breathing curves with different degree of (ir)regularity. The corresponding end-inspiration 4DCT images were reconstructed exemplarily amplitude-based. In addition to a (i) regular breathing curve, the selected scenarios were (ii) irregular breathing frequency, (iii) irregular breathing amplitude, and (iv) a combination of ii and iii.

2.6. Selection of challenging cases and expert rater study

Similar to Werner et al. [22], an expert rater study was designed to evaluate the image quality.

Thirty out of the 129 respiratory curves were selected based on expert knowledge of two physicists (JS, CH) specialized in 4DCT artifacts. The selection criteria included different types of pronounced breathing irregularities (occurrence of breathing pauses, strong variability in breathing frequency, and/or variations in amplitude or baseline drifts). In previous phantom study [22,24], we have shown in a direct comparison of conventional 4DCT and i4DCT that these previously mentioned breathing patterns lead to artifacts. In addition, the reconstructed images had to cover the entire lung area to be included in the rater study; this led to exclusion of 8/129 (6%) breathing curves. Fig. 1 shows a comparison of two patients with a regular and an irregular breathing pattern, respectively. The breathing curves for all 30 patients selected for the rater study can be seen in the supplementary material.

The rating was performed by ten clinicians (five medical physicists, five physicians). All $30 \times 2 = 60$ scans (30 patients, amplitude- and phase-based reconstruction) were presented as animations in sagittal and coronal views to each rater. The data was pseudonymized after reconstruction and presented in shuffled order. The scans were evaluated on a 5-score scale, ranging from five (*artifact-free image,* all anatomical structures can be recognized clearly) to three (*moderate artifacts,* still usable with caution for radiotherapy treatment planning) to one (*bad quality,* inacceptable loss of relevant information). The corresponding scoring guidelines and examples can be found in the supplementary material and in [22].

Statistical significance of differences between amplitude-based (AB) and phase-based (PB) reconstruction (physicians and physicists pooled) as well as differences between the observer groups (AB and PB pooled) was tested using the Wilcoxon signed-rank test with Bonferroni correction at a significance level of 5%.

2.7. Projection data coverage and beam-on time analysis

To evaluate whether the performance measures derived *in-silico* [23] match the actual numbers for the considered patient cohort, the so-called projection data coverage (β in [23]) was analyzed. Projection data coverage was computed for each patient based on the patient's breathing curve acquired during 4DCT scanning. The computation consisted of three steps. First, covering all breathing cycles acquired during the entire 4DCT scan of the patient, the median end-exhalation signal value A_e and the median end-inhalation signal value A_i were computed. Based on A_e,A_i, inhalation and exhalation coverage values β_e^z, β_i^z were computed for each beam-on period and the corresponding z-position, respectively. Let $[A^z_{e,min}, A^z_{e,max}]$ denote the interval of the breathing signal values that were covered during exhalation of the patient during the beam-on time at couch position z, β_e^z was derived as

$$\beta_e^z = \frac{min\left\{A_i, A^z_{e,max}\right\} - max\{A_e, A^z_{e,min}\}}{A_i - A_e}$$

for overlapping intervals $\left[\widetilde{A}_e,\ \widetilde{A}_i\right]$ and $[A^z_{e,min},\ A^z_{e,max}]$, and $\beta_e^z = 0$ otherwise. β_i^z is similarly defined, but taking into account only inhalation breathing signal values acquired during beam-on at couch position z. The reported inhalation projection coverage for the patient then corresponded to the median of the β_i^z values obtained for the different z-positions of the scan (and similar for exhalation projection coverage). Further details and illustrations were given in [23].

Coverage values were computed and evaluated for each scan of the entire cohort (129 scans) and separately for the 'challenging cases' subset. Finally, beam-on times were analyzed to evaluate to which degree breathing irregularity leads to a prolongation of the i4DCT beam-on time and imaging dose, respectively. Statistical significance of differences in coverage or beam-on time was tested using the Wilcoxon rank-sum test with Bonferroni correction.

3. Results

3.1. Exemplary cases

Strong variations in frequency resulting in missing projection data artifacts cannot be observed (see Fig. 2ii). It can be seen, that the beam-on period ranges from peak to peak even though peaks are not regularly positioned. The loss of information due to the underlying mismatch of breathing frequency and scan parameters for conventional 4DCT protocols was avoided by individually adjusting both the starting point and the length of the beam-on times at the different z-positions to the patient's breathing pattern.

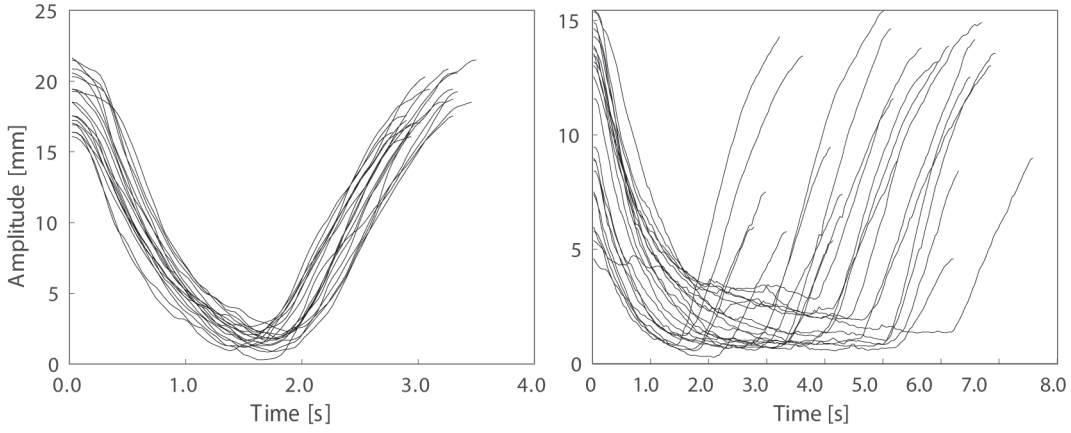

Fig. 1. Exemplary plot to illustrate the difference between regular (left) and irregular (right) breathing curves. The plots contain the individual breaths of a patient's respiration as acquired during the CT scan. The greater variation in amplitude and frequency of the irregular breathing curve is clearly recognizable.

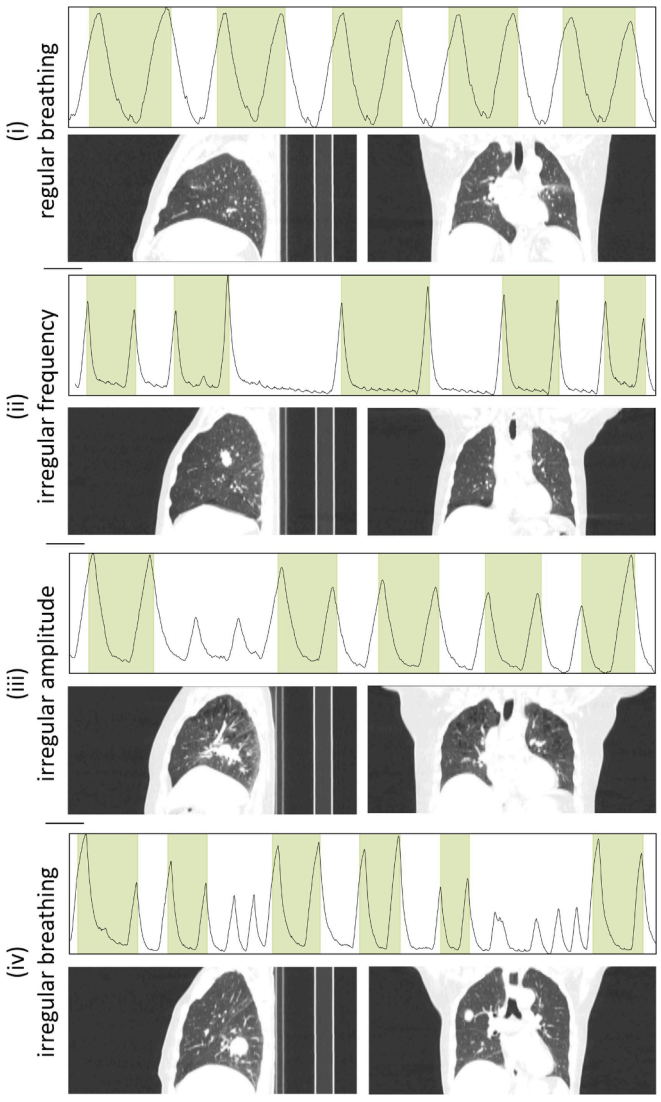

Fig. 2. Breathing curves with beam-on periods (shaded/green) and corresponding images for four different exemplary cases scanned with i4DCT: (i) regular breathing curve, (ii) irregular breathing frequency, (iii) irregular breathing amplitude, and (iv) a combination of the before-mentioned irregularities. Resulting image quality is shown at maximum inhalation for amplitude-based reconstruction in sagittal and coronal views. Abscissa: Time [a.u.], Ordinate: Amplitude [a.u.]. (For interpretation of the references to colour in this figure legend, the reader is referred to the web version of this article.)

Artifacts like double or incomplete structures caused by strong variations in breathing cycle amplitude cannot be observed when using i4DCT despite pronounced breathing amplitude outliers with lower amplitude (see Fig. 2iii). These outliers were detected by the algorithm and the scan was not enabled during these cycles. Thus inappropriate or missing projection data resulting in artifacts were avoided.

Even for a combination of both types of irregularities (see Fig. 2iv) neither incomplete or double structures nor missing data artifacts could be observed. This was achieved by the individual adjustment of the scan time at the individual z-positions according to the varying breathing frequency and the exclusion of breathing cycles with significantly smaller amplitudes.

3.2. Expert rater study

A total of 78% and 63% (AB and PB, respectively) of the images were rated with 4 and 5, i.e., no or only minimal artifacts were observed despite the presence of pronounced breathing irregularities. Strong artifacts that would lead to a total loss of relevant image information only occurred in 2% and 9% of the cases (AB and PB, respectively; rated with a score of 2). No image was rated with 1 (see Fig. 3).

The analysis of the two observer groups showed that physicians on average rate the image quality lower than physicists (mean rating AB 4.3 vs. 4.0; PB 4.0 vs. 3.7, $p < 0.001$). Moreover, AB achieved significantly higher image quality than PB (mean rating AB: 4.1, PB: 3.8, $p < 0.001$).

3.3. Projection data coverage and beam-on time analysis

The mean projection data coverage for the entire population was 92% ± 8% (median 93%) for inhalation and 93% ± 7% (median 94%) for exhalation. The comparison of the projection data coverage for the subset of the challenging breathing curves (inhalation: 89% ± 9%, median 90%; exhalation: 90% ± 7%, median 93%) and the remaining patients (inhalation: 93% ± 7%, median 94%; exhalation: 94% ± 5%, median 94%) revealed a small but significant decrease of the coverage values for the challenging curves (inhalation: $p = 0.02$; exhalation: $p = 0.02$). The average beam-on time per couch position was 4.9 ± 1.6 s (median 4.5 s) for the entire patient cohort. The time slightly increased for the challenging breathing curves (5.1 ± 1.7 s, median 4.6 s), but differences compared to the remaining patients (4.9 ± 1.6 s, median 4.5 s) were not significant ($p = 0.64$).

4. Discussion

In the current work, the first clinical, i.e., patient data, acquired with the first commercial implementation of i4DCT was evaluated. It adds the clinical component to the previously published i4DCT *in-silico* and phantom studies [22–24]. These studies have demonstrated that when i4DCT was used, irregular breathing had less negative impact on image quality and led to less image artifacts than other commercial 4DCT scanning modes [22,24]. The presented results for the clinical data were in good agreement with those of the phantom study [22] for both the rater study and the analysis of the projection data coverage.

Comparing the numbers for the i4DCT projection data coverage analysis and those for the prior *in-silico* study revealed very high agreement for both the entire patient cohorts (clinical data: median inhalation coverage 93%, exhalation 94%; *in-silico* study: median coverage of 93% [23]) and considered subcohorts of challenging breathing curves (clinical data: inhalation 90%, exhalation 93%; *in-silico* study: 90%). In contrast, for standard spiral 4DCT scanning, the *in-silico* study revealed a projection data coverage of only 82% for irregular breathing curves. The improved projection data coverage by i4DCT was the result of individually adjusting the starting point and the length of the beam-on periods at the different z-positions to the patient's breathing pattern during scanning. This, in turn, counteracts common artifacts.

The rater study was performed to qualitatively measure the image quality of the i4DCT patient data. For patients, it was not possible to directly compare i4DCT to conventional 4DCT due to a) the dose burden to the patient and b) the fact that a patient would not be able to reproduce the exact same breathing pattern for both scans. Nevertheless, through adequate selection of patients with pronounced breathing irregularities in accordance with the selection in [22], it was possible to compare the results of the present and the phantom study [22].

The distribution of expert ratings for the reconstructed clinical

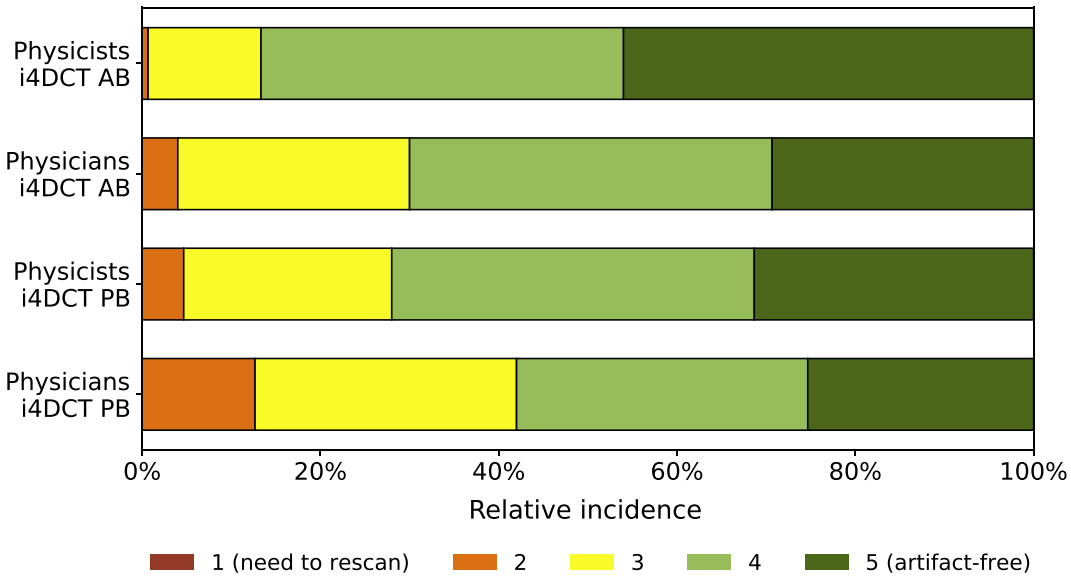

Fig. 3. Summary of the expert rater study results. The relative incidence for both reconstruction modes (amplitude- and phase-based) and observer groups (physicians and physicists) is visualized for each score of the 5-level image quality score. No image was rated with one.

images of the 'challenging cases' subcohort agreed well with the i4DCT results of the recent phantom study [22] that compared image quality for i4DCT and conventional spiral 4DCT. The rater study thereby supported that, in the presence of breathing irregularities, the i4DCT algorithm was able to significantly improve image quality in comparison to conventional 4DCT scanning.

Even with the new algorithm, artifact-free images could not be reconstructed for all possible breathing curves (AB: 38%, PB: 28% scored with five). Mismatches in the phase or displacement at adjacent table positions may still occur in case of very pronounced breathing irregularities and can still manifest as artifacts (images rated with 2 or 3, examples in supplementary material). If a patient has a longer breathing cycle than a defined time (e.g. t_{max} = 18.5 s, depends on patient's breathing frequency), this still leads to artifacts, which are due to missing projection data in certain breathing phases. Overall, however, the achieved image quality showed very good results especially considering that only challenging breathing curves were used in the rater study (AB: 78%, PB: 63% rated with $\geq$4). Similar results were achieved in the phantom study (AB: 74%, PB: 53% rated with $\geq$4). Thus, the encouraging results of the phantom study [22] were well reproduced in the present patient analysis. In comparison, conventional 4DCT was only able to show 13% and 5%, respectively, of (nearly) artifact-free images in the phantom study for amplitude- and phase-based reconstruction [22]. The i4DCT patient and phantom ratings also agreed well for the fraction of scans that were considered not appropriate for treatment planning (rated with $\leq$2). For i4DCT, the fraction was 2% (patient analysis) and 5% (phantom study) for amplitude-based reconstruction. Conventional spiral 4DCT was associated with a significantly higher ratio of 58% in the phantom study [22].

Yamamoto et al. [14] warned in an early 4DCT image quality rating study that the frequency and magnitude of artifacts in clinically used 4DCT scans was disturbingly high. They reported that up to 90% of the considered scans had at least one image artifact. A similarly high number was published by Keall et al. [15], investigating consecutive patient scans. 13 of 15 scans (~85%) showed obvious artifacts. In a more recent retrospective analysis of 50 patients who received a 4DCT, Wulfhekel et al. [25] also reported that 75% of the images were corrupted by artifacts. Comparing these numbers with those obtained in the present study, a significant improvement in image quality was achieved by i4DCT, especially when taking into account that, in contrast to previously published results, the expert rating was only performed for patients with pronounced breathing irregularity.

Several authors indicated that the reduction in artifacts also reduces the delineation and dose calculation errors associated with these artifacts [10,15,17,20]. We therefore assume that the artifact reduction achieved by i4DCT will also lead to a reduction in the before mentioned errors.

Unfortunately, the algorithm is currently only supported by two systems, including the RGSC system. However, in comparison to other commercially used systems (e.g. breathing belts [26,27], spirometry [28]), the RGSC has the advantages of not affecting patient's breathing and a high patient comfort. More information of the RGSC can be found in Shi et al. [29].

The present data demonstrated that AB achieves significantly higher image quality than PB ($p < 0.001$). This confirms the previously published results that PB is more susceptible to breathing irregularities than AB [13,27,30–32].

In summary, the new i4DCT algorithm provided good image quality in terms of artifact reduction and improved projection data coverage for clinical data, even for patients with irregular breathing curves, due to the patient-specific adaptation of the scan parameters prior to scanning, online analysis of the respiratory signal during scanning and signal- and data coverage-driven adaptation of beam-on periods.

Declaration of Competing Interest

The authors declare the following financial interests/personal relationships which may be considered as potential competing interests: The Universitätsklinikum Erlangen and also the Department of Radiation Oncology have institutional research grants with Siemens Healthcare GmbH. RW was further supported by a research grant from Siemens Healthcare GmbH and DFG grant WE 6197/2-1. AS, SF, CH are with Siemens Healthcare GmbH.

Acknowledgements

We thank the following members of our department for participating in our rater study: Daniel Popp, Tim-Oliver Sauer, Rosalind Perrin, Claudia Schweizer, Hanno Zoske, Johannes Roesch, Philipp Schubert and Allison Müller.

The presented work was performed by Juliane Szkitsak in partial fulfillment of the requirements for obtaining the degree “Dr. rer. biol. hum.” at the Friedrich-Alexander-Universität (FAU).

All procedures performed were in accordance with the ethical standards of the institutional research committee, the local laws, and with the 1964 Helsinki declaration and its later amendments.

Appendix A. Supplementary data

Supplementary data to this article can be found online at https://doi.org/10.1016/j.phro.2021.09.005.

References

[1] Brennan D, Schubert L, Diot Q, Castillo R, Castillo E, Guerrero T, et al. Clinical validation of 4-dimensional computed tomography ventilation with pulmonary function test data. Int J Radiat Oncol Biol Phys 2015;92:423–9. https://doi.org/10.1016/j.ijrobp.2015.01.019.

[2] Keall PJ, Mageras GS, Balter JM, Emery RS, Forster KM, Jiang SB, et al. The management of respiratory motion in radiation oncology report of AAPM Task Group 76a). Med Phys 2006;33:3874–900. https://doi.org/10.1118/1.2349696.

[3] Landberg T, Chavaudra J, Dobbs J, Gerard J-P, Hanks G, Horiot J-C, et al. Report 62. J ICRU 2016;os32. https://doi.org/10.1093/jicru/os32.1.Report62.

[4] Underberg RWM, Lagerwaard FJ, Cuijpers JP, Slotman BJ, van Sörnsen de Koste JR, Senan S. Four-dimensional CT scans for treatment planning in stereotactic radiotherapy for stage I lung cancer. Int J Radiat Oncol Biol Phys 2004;60:1283–90. https://doi.org/10.1016/j.ijrobp.2004.07.665.

[5] Schmitt D, Blanck O, Gauer T, Fix MK, Brunner TB, Fleckenstein J, et al. Technological quality requirements for stereotactic radiotherapy. Strahlenther Onkol 2020;196:421–43. https://doi.org/10.1007/s00066-020-01583-2.

[6] Underberg RW, Lagerwaard FJ, Slotman BJ, Cuijpers JP, Senan S. Benefit of respiration-gated stereotactic radiotherapy for stage I lung cancer: an analysis of 4DCT datasets. Int J Radiat Oncol Biol Phys 2005;62:554–60. https://doi.org/10.1016/j.ijrobp.2005.01.032.

[7] Keall PJ, Starkschall G, Shukla H, Forster KM, Ortiz V, Stevens CW, et al. Acquiring 4D thoracic CT scans using a multislice helical method. Phys Med Biol 2004;49:2053–67. https://doi.org/10.1088/0031-9155/49/10/015.

[8] Werner R, Hofmann C, Mucke E, Gauer T. Reduction of breathing irregularity-related motion artifacts in low-pitch spiral 4D CT by optimized projection binning. Radiat Oncol 2017;12:100. https://doi.org/10.1186/s13014-017-0835-7.

[9] Hertanto A, Zhang Q, Hu Y-C, Dzyubak O, Rimner A, Mageras GS. Reduction of irregular breathing artifacts in respiration-correlated CT images using a respiratory motion model. Med Phys 2012;39:3070–9. https://doi.org/10.1118/1.4711802.

[10] Persson GF, Nygaard DE, Brink C, Jahn JW, Munck af Rosenschöld P, Specht L, et al. Deviations in delineated GTV caused by artefacts in 4DCT. Radiother Oncol 2010;96:61–6. https://doi.org/10.1016/j.radonc.2010.04.019.

[11] Pan T, Sun X, Luo D. Improvement of the cine-CT based 4D-CT imaging. Med Phys 2007;34:4499–503. https://doi.org/10.1118/1.2794225.

[12] Bernatowicz K, Keall P, Mishra P, Knopf A, Lomax A, Kipritidis J. Quantifying the impact of respiratory-gated 4D CT acquisition on thoracic image quality: A digital phantom study. Med Phys 2015;42:324–34. https://doi.org/10.1118/1.4903936.

[13] Mutaf YD, Antolak JA, Brinkmann DH. The impact of temporal inaccuracies on 4DCT image quality. Med Phys 2007;34:1615–22. https://doi.org/10.1118/1.2717404.

[14] Yamamoto T, Langner U, Loo Jr BW, Shen J, Keall PJ. Retrospective analysis of artifacts in four-dimensional CT images of 50 abdominal and thoracic radiotherapy patients. Int J Radiat Oncol Biol Phys 2008;72:1250–8. https://doi.org/10.1016/j.ijrobp.2008.06.1937.

[15] Keall PJ, Vedam SS, George R, Williamson JF. Respiratory regularity gated 4D CT acquisition: concepts and proof of principle. Australas Phys Eng S 2007;30:211–20. https://doi.org/10.1007/BF03178428.

[16] Watkins WT, Li R, Lewis J, Park JC, Sandhu A, Jiang SB, et al. Patient-specific motion artifacts in 4DCT. Med Phys 2010;37:2855–61. https://doi.org/10.1118/1.3432615.

[17] Langner UW, Keall PJ. Prospective displacement and velocity-based cine 4D CT. Med Phys 2008;35:4501–12. https://doi.org/10.1118/1.2977539.

[18] Rietzel E, Pan T, Chen GT. Four-dimensional computed tomography: image formation and clinical protocol. Med Phys 2005;32:874–89. https://doi.org/10.1118/1.1869852.

[19] Werner R, Gauer T. Reference geometry-based detection of (4D-)CT motion artifacts: a feasibility study. In: Ourselin S, Styner MA, editors. Medical imaging 2015: Imaging processing. SPIE. 2015;9413:0S1-7. https://doi.org/10.1117/12.2075853.

[20] Castillo SJ, Castillo R, Castillo E, Pan T, Ibbott G, Balter P, et al. Evaluation of 4D CT acquisition methods designed to reduce artifacts. J Appl Clin Med Phys 2015;16:23–32. https://doi.org/10.1120/jacmp.v16i2.4949.

[21] Sentker T, Schmidt V, Ozga A-K, Petersen C, Madesta F, Hofmann C, et al. 4D CT image artifacts affect local control in SBRT of lung and liver metastases. Radiother Oncol 2020;148:229–34. https://doi.org/10.1016/j.radonc.2020.04.006.

[22] Werner R, Szkitsak J, Sentker T, Madesta F, Schwarz A, Fernolendt S, et al. Comparison of intelligent 4D CT sequence scanning and conventional spiral 4D CT: a first comprehensive phantom study. Phys Med Biol 2021;66:015004. https://doi.org/10.1088/1361-6560/abc93a.

[23] Werner R, Sentker T, Madesta F, Gauer T, Hofmann C. Intelligent 4D CT sequence scanning (i4DCT): Concept and performance evaluation. Med Phys 2019;46:3462–74. https://doi.org/10.1002/mp.13632.

[24] Werner R, Sentker T, Madesta F, Schwarz A, Vornehm M, Gauer T, et al. Intelligent 4D CT sequence scanning (i4DCT): First scanner prototype implementation and phantom measurements of automated breathing signal-guided 4D CT. Med Phys 2020;47:2408–12. https://doi.org/10.1002/mp.14106.

[25] Wulfhekel E, Grohmann C, Gauer T, Werner R. EP-1743: Compilation of a database for illustration and automated detection of 4DCT motion artifacts. Radiother Oncol 2014;111:S266. https://doi.org/10.1016/S0167-8140(15)31861-2.

[26] Li XA, Stepaniak C, Gore E. Technical and dosimetric aspects of respiratory gating using a pressure-sensor motion monitoring system. Med Phys 2006;33:145–54. https://doi.org/10.1118/1.2147743.

[27] Guckenberger M, Weininger M, Wilbert J, Richter A, Baier K, Krieger T, et al. Influence of retrospective sorting on image quality in respiratory correlated computed tomography. Radiother Oncol 2007;85:223–31. https://doi.org/10.1016/j.radonc.2007.08.002.

[28] Low DA, Nystrom M, Kalinin E, Parikh P, Dempsey JF, Bradley JD, et al. A method for the reconstruction of four-dimensional synchronized CT scans acquired during free breathing. Med Phys 2003;30:1254–63. https://doi.org/10.1118/1.1576230.

[29] Shi C, Tang X, Chan M. Evaluation of the new respiratory gating system. Precis Radiat Oncol 2017;1:127–33. https://doi.org/10.1002/pro6.34.

[30] Lu W, Parikh PJ, Hubenschmidt JP, Bradley JD, Low DA. A comparison between amplitude sorting and phase-angle sorting using external respiratory measurement for 4D CT. Med Phys 2006;33:2964–74. https://doi.org/10.1118/1.2219772.

[31] Vedam SS, Keall PJ, Kini VR, Mohan R. Determining parameters for respiration-gated radiotherapy. Med Phys 2001;28:2139–46. https://doi.org/10.1118/1.1406524.

[32] De Ruysscher D, Faivre-Finn C, Moeller D, Nestle U, Hurkmans CW, Le Péchoux C, et al. European Organization for Research and Treatment of Cancer (EORTC) recommendations for planning and delivery of high-dose, high precision radiotherapy for lung cancer. Radiother Oncol 2017;124:1–10. https://doi.org/10.1016/j.radonc.2017.06.003.